# Particle Physics Study Report 2 (7/11)

Minjae Kim

July 13, 2026

## 1 Introduction

This study report presents a formulation and application of Effective Field Theory (EFT) through amplitude matching. We begin with formulation EFT by separating light and heavy particle fields and integrating out the heavy particle field to construct a low-energy effective Lagrangian. To determine which terms must be retained at a fixed precision, we derive a power-counting formula based on dimensional analysis, loop order, and the number of derivatives in each term. As an explicit example, we consider a toy model with spontaneous symmetry breaking in a complex scalar field. After constructing the most general effective Lagrangian for the Goldstone boson up to the desired order, we compute the $\xi\xi \to \xi\xi$ scattering amplitude in both the high-energy theory and the EFT. By matching the two amplitudes, we determine the Wilson coefficients $c_1$ and $c_2$ up to one-loop precision. Finally, we discuss the general significance of EFT.

The theoretical framework and analytical derivations presented in this study report are based on the following foundational texts: Chapters 11 and 12 of Peskin and Schroeder's *An Introduction to Quantum Field Theory*; Chapters 21, 29, 30, 31, and 32 of Srednicki's *Quantum Field Theory*; and Chapters 1, 2, 3, and 7 of Burgess's *Introduction to Effective Field Theory*.

## 2 Formulation of Effective Field Theory

When an underlying high-energy theory (or UV theory) is known, it is mathematically efficient to construct a low-energy approximation valid to the specific energy domain of interest. This allows the formalism to isolate the dominant interaction terms. For instance, heavy fields dynamically decouple when the interaction energy is significantly smaller than their masses. The resulting framework is termed an Effective Field Theory (EFT). It must be emphasized that EFT is not merely a practical approximation scheme for a known full theory; its profound significance will be detailed in Chapter 5.

A traditional, physically intuitive approach to formulating an EFT involves introducing a momentum cutoff $\Lambda$ and explicitly integrating out the high-energy modes. However, this method exhibits severe technical deficiencies: it produces intractable multi-scale integrals and explicitly violates underlying gauge and translational symmetries. Consequently, this report bypasses the cutoff scheme and formulates EFT directly utilizing Dimensional Regularization (DIMREG).

Consider the general structure of a full high-energy theory containing light particle fields $\phi$ and heavy particle fields $\Phi$:

$$S[\phi, \Phi] = \int d^d x \mathcal{L}(\phi, \Phi) \tag{1}$$

The physically relevant regime occurs when their respective masses $m$ and $M$, and the characteristic interaction energy $E$, satisfy the hierarchy:

$$m \lesssim E \ll M \tag{2}$$

This scale separation is critical: the energy is sufficient to excite light particles as on-shell states (external lines), whereas heavy particles are confined to quantum fluctuations (internal lines). The generating functional for connected diagrams, coupled to external sources $j$ and $J$, is defined as:

$$e^{iW[j,J]} = \int \mathcal{D}\phi \mathcal{D}\Phi \, e^{i\left[S[\phi,\Phi] + \int d^d x j\phi + \int d^d x J\Phi\right]} \tag{3}$$

To restrict the analysis to low-energy observables with only light external lines, we set the source current $J$ for the heavy field to zero. Thus, we define the effective generating functional $W_{\text{eff}}[j]$ which exclusively sources the light fields:

$$e^{iW_{\text{eff}}[j]} = \int \mathcal{D}\phi \mathcal{D}\Phi \, e^{i\left[S[\phi,\Phi] + \int d^d x j\phi\right]} \tag{4}$$

The path integration over the heavy particle field $\Phi$ can be factored out from the original action to define the Wilson action $S_{\text{eff}}[\phi]$ and its effective Lagrangian $\mathcal{L}_{\text{eff}}(\phi)$:

$$e^{iS_{\text{eff}}[\phi]} = \int \mathcal{D}\Phi \, e^{iS[\phi,\Phi]} \tag{5}$$

$$S_{\text{eff}}[\phi] = \int d^d x \mathcal{L}_{\text{eff}}(\phi) \tag{6}$$

Why can Wilson action be expressed by the spacetime integration of a certain effective Lagrangian? This is because each integration over heavy particle field $\Phi$ can be treated as treated locally from the $p/M$ expansion. This locality is a direct consequence of the Heisenberg uncertainty principle ($\Delta p \Delta x \geq \hbar/2$). Exciting a heavy virtual particle requires an immense energy fluctuation ($\Delta p \sim M$), which dynamically constrains its allowed spacetime propagation to an infinitesimally short duration ($\Delta x \sim 1/M$). From the perspective of a low-energy observer ($E \ll M$), this unresolvable propagation collapses entirely into a single spacetime point, manifesting mathematically as a local contact interaction.

Utilizing this Wilson action, the final exact expression for the effective generating functional $W_{\text{eff}}[j]$ takes the form:

$$e^{iW_{\text{eff}}[j]} = \int \mathcal{D}\phi \, e^{i\left[S_{\text{eff}}[\phi]+\int d^d x j \phi\right]} \tag{7}$$

Now our goal has been reduced by achieving the coefficients of the effective Lagrangian, which is called the Wilson coefficient. The formulation of the EFT Lagrangian via amplitude matching systematically proceeds through the following four steps:

**Step 1: Expansion of the EFT Lagrangian** The procedure begins by defining the foundational expansion of the EFT. The desired theoretical precision is fixed to a multiple expansion: for example, specific power of the momentum-to-mass ratio $(p/M)$, and powers of coupling constant $\lambda$. Based on this predefined threshold, only the terms that fall strictly within this order are selected and retained to construct the effective Lagrangian.

**Step 2: High-Energy Theory Amplitude Calculation** The number of effective terms isolated in Step 1 dictates the degrees of freedom, which correspond to the unknown Wilson coefficients. To constrain these unknowns, appropriate target scattering amplitude are selected. These amplitudes are then explicitly calculated within the original high-energy framework, employing Dimensional Regularization (DIMREG) to systematically manage and renormalize any divergences.

**Step 3: EFT Amplitude Calculation** Utilizing the selected effective terms and parameterized by their unknown Wilson coefficients, the identical scattering amplitudes chosen in Step 2 are computed within the low-energy EFT framework.

**Step 4: Matching** The exact matching condition is enforced by equating the renormalized amplitudes derived from the high-energy theory and the EFT. By algebraically comparing the two expressions order-by-order, the explicit physical values of the Wilson coefficients are definitively extracted.

# 3 Power Counting

How do we systematically determine which terms survive within the targeted precision threshold in Step 1? This problem introduces the absolute necessity for *power counting*. Without a mathematical framework to evaluate the parametric suppression of an infinite tower of possible term combinations, systematic approach is impossible. Power counting provides the exact algebraic mechanism to calculate the suppression order of each term, dictating precisely which terms must be included to achieve the desired accuracy.

Power counting is an efficient mechanism for systematically evaluating the parametric scale of each Feynman diagram using specific dimensionful quantities. To execute this, every variable within the Lagrangian must be assigned a formal mass dimension. Assuming natural units ($\hbar = c = 1$), and letting $\phi$ and $\psi$ denote canonically normalized bosonic and fermionic fields, the dimensional assignments are:

$$[S] = 0 \tag{8}$$
$$[x] = -1 \tag{9}$$
$$[\partial] = 1 \tag{10}$$
$$[\mathcal{L}] = d \tag{11}$$
$$[m] = 1 \tag{12}$$
$$[\phi] = \frac{d}{2} - 1 \tag{13}$$
$$[\psi] = \frac{d}{2} - \frac{1}{2} \tag{14}$$

To formalize the scaling analysis, we introduce the dimensionful scaling factors $\mathcal{L}_s$, $M$, $\phi_s$, and $\psi_s$, which possess mass dimensions identical to $\mathcal{L}$, $\partial$, $\phi$, and $\psi$, respectively. By utilizing these scaling factors to factor out the dimensions of their corresponding quantities, the dimensionally regularized effective Lagrangian can be expressed exactly in terms of dimensionless Wilson coefficients $\hat{c}_n$:

$$\mathcal{L}_{\text{eff}} = \frac{\mathcal{L}_s}{M^2 \phi_s^2} \mathcal{L}_{b0} + \frac{\mathcal{L}_s}{M \psi_s^2} \mathcal{L}_{f0} + \mathcal{L}_s \sum_n \frac{\hat{c}_n}{M^{d_n}} \mathcal{O}_n \left( \frac{\phi(x)}{\phi_s}, \frac{\psi(x)}{\psi_s} \right) \tag{15}$$

$$= \frac{\mathcal{L}_s}{M^2 \phi_s^2} \mathcal{L}_{b0} + \frac{\mathcal{L}_s}{M \psi_s^2} \mathcal{L}_{f0} + \mathcal{L}_s \sum_n \frac{\hat{c}_n}{M^{d_n} \phi_s^{b_n} \psi_s^{f_n}} \mathcal{O}_n(\phi(x), \psi(x)) \tag{16}$$

Here, $\mathcal{L}_{b0}, \mathcal{L}_{f0}$ designate the bosonic and fermionic free-field Lagrangians, while $d_n$, $b_n$, and $f_n$ respectively denote the number of derivatives, bosonic fields, and fermionic fields contained within the $n$-th interaction term.

Physically, the scales $\phi_s$ and $\psi_s$ map to the vacuum expectation values associated with spontaneous symmetry breaking. The scale $M$, which normalizes the derivatives, rigorously represents the mass of the integrated-out high-energy field. The reason for this is justified as the following. Every derivative in the effective Lagrangian translates to an external momentum insertion in the amplitude. Crucially, these momentum insertions originate exclusively from the Taylor expansion of the heavy-field propagator, $1/(p^2 + M^2)$. Through this expansion, every low-energy momentum $p$ is strictly coupled to the heavy mass scale as the ratio $p/M$. Therefore, the scale $M$ must match to each derivative term $\partial$. Lastly, $\mathcal{L}_s$ characterizes the overall energy density of the system in the limit where all physical quantities are of the same order of magnitude as their respective scaling factors.

Now, consider an arbitrary connected Feynman diagram possessing $E_b$ and $E_f$ bosonic and fermionic external lines, $I_b$ and $I_f$ bosonic and fermionic internal lines (propagators), and $V_n$ vertices of the $n$-th interaction term. From the topological properties of the graph, the following identities hold:

$$2I_b + E_b = \sum_n b_n V_n \tag{17}$$

$$2I_f + E_f = \sum_n f_n V_n \tag{18}$$

Furthermore, counting the number of loops with momenta and constraints (where $L$ is the number of loops, total internal lines is $I_b + I_f$, and total vertices is $\sum_n V_n$), we find:

$$L = I_b + I_f - \left( \sum_n V_n - 1 \right) \tag{19}$$

For intermediate algebraic simplicity, we suppress the explicit dimensionful scaling factors $(\mathcal{L}_s, M, \phi_s, \psi_s)$. The integral dimensionally scales as:

$$\begin{aligned} &\int \left( \frac{d^d p}{(2\pi)^d} \right)^L \frac{p^{\sum_n d_n V_n}}{(p^2 + p_s^2)^{I_b} (\not{p} + p_s)^{I_f}} \\ &\sim \int \left( \frac{d^d p}{(2\pi)^d} \right)^L \frac{p^{\sum_n d_n V_n}}{(p^2 + p_s^2)^{I_b + I_f/2}} \\ &\sim \frac{1}{(4\pi)^{dL/2}} \, p_s^{dL + \sum_n d_n V_n - 2I_b - I_f} \\ &\xrightarrow{d \to 4} \frac{1}{(4\pi)^{2L}} \, p_s^{4L + \sum_n d_n V_n - 2I_b - I_f} \end{aligned} \tag{20}$$

Here, $p_s$ denotes the characteristic dynamical energy scale that dominates the integral. If the light masses and external momenta are on a comparable scale, $p_s$ represents the unified scale. In the extreme relativistic limit, $p_s$ is simply identified with the characteristic external momentum.

Restoring all suppressed dimensional scaling factors for the vertices and propagators, and applying equations (17), (18), and (19), the parametric scale of the diagram is given by:

$$\mathcal{A}(E, L, \{d_n, V_n\}) \sim \tag{21}$$

$$\frac{1}{(4\pi)^{2L}} \, p_s^{4L + \sum_n d_n V_n - 2I_b - I_f} \left( \frac{M^2 \phi_s^2}{\mathcal{L}_s} \right)^{I_b} \left( \frac{M \psi_s^2}{\mathcal{L}_s} \right)^{I_f} \prod_n \left( \frac{\mathcal{L}_s}{M^{d_n} \phi_s^{b_n} \psi_s^{f_n}} \right)^{V_n} \tag{22}$$

$$= \mathcal{L}_s \left( \frac{1}{\phi_s} \right)^{E_b} \left( \frac{1}{\psi_s} \right)^{E_f} \left( \frac{p_s M}{4\pi \sqrt{\mathcal{L}_s}} \right)^{2L} \left( \frac{p_s}{M} \right)^{2 - E_f/2 + \sum_n (d_n + f_n/2 - 2) V_n} \tag{23}$$

This expression is the final power counting formula. Before we apply this formula to a specific example, it provides profound insights into the validity of perturbative analysis in EFT. This is because the fundamental condition of perturbation theory is that higher-order corrections must become smaller. If the amplitude grows as the diagram becomes more complex (i.e., higher loops and more vertices), it becomes impossible to achieve a given precision goal by evaluating a finite number of diagrams.

First, the constraints on the dimensionless Wilson coefficients $\hat{c}_n$ are significantly relaxed compared to a fundamental high-energy theory. Even if $\hat{c}_n \sim \mathcal{O}(1)$, the low-energy condition of the EFT naturally suppresses the contributions from higher-order terms according to the power counting formula. Thus, the small physical momenta constrain the complexity of the effective field theory, making the perturbative analysis valid without requiring artificially small coupling constants.

Second, the formula allows us to identify potentially dangerous diagrams that need a case-by-case basis. As a diagram becomes more complex, both the number of loops $L$ and the number of higher-dimensional vertices $V_n$ increase. If the characteristic momentum $p_s$ is sufficiently low—specifically, $p_s \ll M$ and $p_s \ll 4\pi\sqrt{\mathcal{L}_s}/M$—the convergence of the perturbative expansion is guaranteed, provided that the last two exponents in equation (23) grows with increasing $L$ and $V_n$. This condition is generally satisfied, except in the specific cases where the coefficient of $V_n$, given by $(d_n + f_n/2 - 2)$, is negative. Those finite exceptions must be treated delicately.

# 4 Toy Model Example

A representative case for demonstrating the EFT formalism is the toy model of spontaneous symmetry breaking involving a complex scalar field. The complete high-energy Lagrangian is defined as:

$$\mathcal{L} = -\partial^\mu \phi^\dagger \partial_\mu \phi - \frac{\lambda}{4}(\phi^\dagger \phi - v^2)^2 \tag{24}$$

This model is ideal for the toy model example because spontaneous symmetry breaking naturally isolates a massless light particle (the Goldstone boson) from a massive radial field. Our interest is when the interaction is very weak: $\lambda \ll 1$.

Before initiating the matching procedure, it is necessary to parameterize the field according to its relevant energy scales. To explicitly isolate the Goldstone boson, the complex scalar field $\phi$ is decomposed into two real scalar fields, $\chi$ and $\xi$:

$$\phi = \left(v + \frac{\chi}{\sqrt{2}}\right) e^{i\xi/(\sqrt{2}v)} \tag{25}$$

Then, the goldstone boson $\xi$ has global shift symmetry $\xi(x) \to \xi(x) + c$. Substituting this parameterization, the total Lagrangian is rewritten in a more useful form:

$$\mathcal{L} = -\frac{1}{2}\partial^\mu \chi \partial_\mu \chi - \frac{1}{2}\left(1 + \frac{\chi}{\sqrt{2}v}\right)^2 \partial^\mu \xi \partial_\mu \xi - \frac{\lambda}{4}\left(\sqrt{2}v\chi + \frac{\chi^2}{2}\right)^2 \tag{26}$$

By inspection of the resulting mass terms, the Goldstone boson field $\xi$ is confirmed to be strictly massless, while the heavy radial field $\chi$ acquires a mass of $m_\chi = \sqrt{\lambda}v$. Consequently, the heavy mass scale $M$ integrated out in this EFT matching is identified as $M = \sqrt{\lambda}v$.

The objective of the following sections is to systematically derive the effective Lagrangian (specifically, the Wilson coefficients) for the light Goldstone bosons $\xi$, up to a precision order up to $\mathcal{O}((p_s/M)^6)$ and $\mathcal{O}(\lambda^2)$, applying the previously established 4-step matching protocol.

## 4.1 Expansion of the Effective Lagrangian

Our chosen precision goal is $\mathcal{O}((p_s/M)^6)$. To utilize the power-counting formula (equation (23)), we must map the dimensionful scaling quantities $(\mathcal{L}_s, M, \phi_s)$ to our specific toy model. By comparing the theoretical structures, these parameters are identified as follows:

$$\mathcal{L}_s = \lambda v^4 \tag{27}$$

$$M = \sqrt{\lambda}v \tag{28}$$

$$\phi_s = v \tag{29}$$

Since our precision goal is about $p_s/M$ and $\lambda$, we need to substituting the relations to eliminate $v = M/\sqrt{\lambda}$. Then, the power-counting formula becomes the following as

$$\mathcal{A}(E, L, \{d_n, V_n\}) \sim \frac{p_s^2 M^2}{\lambda} \cdot \left(\frac{\sqrt{\lambda}}{M}\right)^E \cdot \left(\frac{p_s\sqrt{\lambda}}{4\pi M}\right)^{2L} \cdot \left(\frac{p_s}{M}\right)^{\sum_n (d_n - 2)V_n} \tag{30}$$

Our objective is to identify all effective Lagrangian terms up to $\mathcal{O}((p_s/M)^6)$. Each term's corresponding amplitudes doesn't contain any loops, so $L = 0$. Also, trimming out dimensional constraint $M^{4-E}$ make first two factors of power-counting formula give additional $(p_s/M)^2$ influence. Summing up, this imposes the constraint:

$$2 + \sum_n (d_n - 2)V_n \leq 6. \tag{31}$$

Another crucial constraint arises from the symmetries inherited from the high-energy theory. Because $\xi$ possesses a constant shift symmetry, every instance of the field $\xi$ in the effective Lagrangian must be accompanied by a derivative. Furthermore, Lorentz invariance requires that all spacetime indices be fully contracted, meaning any additional derivatives (such as the d'Alembertian $\Box = \partial^\mu \partial_\mu$) must appear in even numbers. Given the inequality above, each valid interaction term must contain a total of 2, 4, or 6 derivatives.

For the $d = 2$ case, the potential candidates are $\Box\xi$ and $\partial^\mu\xi\partial_\mu\xi$. However, the first term $\Box\xi = \partial^\mu\partial_\mu\xi$ is a total derivative. By applying Stokes' theorem, total derivatives evaluate to boundary terms and are thus physically redundant, as the action must remain independent of boundary conditions:

$$\int_M d^4x \partial_\mu V^\mu(x) = \int_{\partial M} d^3x n_\mu V^\mu(x) \tag{32}$$

Therefore, the only remaining term for $d = 2$ is $\partial^\mu\xi\partial_\mu\xi$, which is the kinetic term of the free Lagrangian.

When $d = 4$, a broader set of terms is conceivable:

$$\Box^2\xi, (\Box\xi)^2, \partial^\mu\partial_\nu\xi\partial^\nu\partial_\mu\xi, \partial^\mu\xi\Box\partial_\mu\xi, \partial^\mu\xi\partial_\mu\xi\Box\xi, (\partial^\mu\xi\partial_\mu\xi)^2 \tag{33}$$

The first term, $\Box^2\xi$, is a total derivative and vanishes by the same logic established previously. Because total derivatives can be discarded, we can freely employ integration by parts ($V(x)\partial_\mu W(x) \to -\partial_\mu V(x)W(x)$). Through this technique, the terms $\partial^\mu\partial_\nu\xi\partial^\nu\partial_\mu\xi, \partial^\mu\xi\Box\partial_\mu\xi$, and $\partial^\mu\xi\partial_\mu\xi\Box\xi$ are shown to be equivalent to $(\Box\xi)^2$. Furthermore, via a field redefinition $\xi \to \xi + \delta\xi$, any term containing $\Box\xi$ can be absorbed into the free Lagrangian at the given order $\mathcal{O}(\delta\xi^2)$:

$$S_0[\xi + \delta\xi] = S_0[\xi] + \int d^4x \frac{\delta S_0}{\delta\xi}\delta\xi + \mathcal{O}(\delta\xi^2) \tag{34}$$

$$= S_0[\xi] - \int d^4x \Box\xi\delta\xi + \mathcal{O}(\delta\xi^2) \tag{35}$$

In other words, we can eliminate these terms by imposing the constraint of the free Lagrangian's classical equation of motion, $\Box\xi = 0$. Consequently, the only surviving independent terms with four derivatives is $(\partial^\mu\xi\partial_\mu\xi)^2$.

Lastly, the $d = 6$ case presents many more possible permutations. However, by systematically eliminating total derivatives and applying the equation of motion ($\Box\xi = 0$) via field redefinitions, the only remaining independent terms are $(\partial^\mu\xi\partial_\mu\xi)\Box(\partial^\nu\xi\partial_\nu\xi)$ and $(\partial^\mu\xi\partial_\mu\xi)^3$.

All in all, the most general structure of the effective Lagrangian up to $\mathcal{O}((p_s/M)^6)$ is given below, parameterized by three unknown Wilson coefficients $c_1, c_2, c_3$:

$$\mathcal{L}_{\text{eff}}(\xi) = -\frac{1}{2}\partial^\mu\xi\partial_\mu\xi + \frac{1}{8}c_1(\partial^\mu\xi\partial_\mu\xi)^2 + \frac{1}{4}c_2(\partial^\mu\xi\partial_\mu\xi)\Box(\partial^\nu\xi\partial_\nu\xi) + \frac{1}{48}c_3(\partial^\mu\xi\partial_\mu\xi)^3 \tag{36}$$

### 4.2 High-Energy Theory Amplitude Calculation

The Lagrangian in equation (26) is about the bare quantities $\chi_0, \xi_0, v_0, \lambda_0$, which contain infinities. We introduce Z-factors $Z_\chi, Z_\xi, Z_v, Z_\lambda$ to absorb its divergences: $\chi_0 = \sqrt{Z_\chi}\chi, \xi_0 = \sqrt{Z_\xi}\xi, v_0 = Z_v v, \lambda_0 = Z_\lambda \lambda$. Then the Lagrangian changes with extra counterterms. (There must be the consideration of arbitrary mass parameter $\mu$ in DIMREG procedure, but I will concentrate on it at the last procedure of renormalization.)

$$\mathcal{L}(\chi,\xi) = -\frac{1}{2}|\partial\chi|^2 - \frac{\lambda v^2}{2}\chi^2 - \frac{1}{2}|\partial\xi|^2 - \frac{\lambda v}{2\sqrt{2}}\chi^3 - \frac{\lambda}{16}\chi^4 - \frac{1}{\sqrt{2}v}\chi|\partial\xi|^2 - \frac{1}{4v^2}\chi^2|\partial\xi|^2 \tag{37}$$

$$\mathcal{L}_{ct}(\chi,\xi) = -(Z_\chi - 1)\frac{1}{2}|\partial\chi|^2 - (Z_\lambda Z_v^2 Z_\chi - 1)\frac{\lambda v^2}{2}\chi^2 - (Z_\xi - 1)\frac{1}{2}|\partial\xi|^2 \tag{38}$$

$$- (Z_\lambda Z_v Z_\chi^{3/2} - 1)\frac{\lambda v}{2\sqrt{2}}\chi^3 - (Z_\lambda Z_\chi^2 - 1)\frac{\lambda}{16}\chi^4 \tag{39}$$

$$- (Z_v^{-1} Z_\chi^{1/2} Z_\xi - 1)\frac{1}{\sqrt{2}v}\chi|\partial\xi|^2 - (Z_v^{-2} Z_\chi Z_\xi - 1)\frac{1}{4v^2}\chi^2|\partial\xi|^2 \tag{40}$$

Those are the Feynman rules for our high-energy theory.

| **Diagram** | **Lagrangian Term** | **Feynman Rule** |
|---|---|---|
| 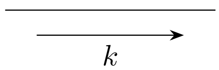 | $-\frac{1}{2}\lvert\partial\chi\rvert^2 - \frac{\lambda v^2}{2}\chi^2$ | $\frac{-i}{k^2 + \lambda v^2 - i\epsilon}$ |
| 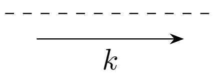 | $-\frac{1}{2}\lvert\partial\xi\rvert^2$ | $\frac{-i}{k^2 - i\epsilon}$ |
| 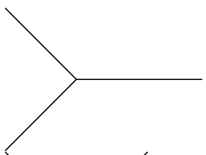 | $-\frac{\lambda v}{2\sqrt{2}}\chi^3$ | $-i\frac{3\lambda v}{\sqrt{2}}$ |
| 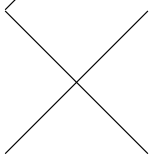 | $-\frac{\lambda}{16}\chi^4$ | $-i\frac{3\lambda}{2}$ |
| 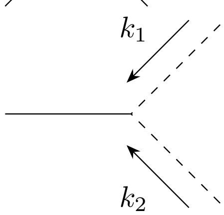 | $-\frac{1}{\sqrt{2}v}\chi\lvert\partial\xi\rvert^2$ | $i\frac{\sqrt{2}}{v}(k_1 \cdot k_2)$ |
| 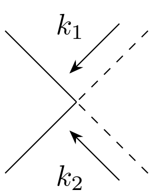 | $-\frac{1}{4v^2}\chi^2\lvert\partial\xi\rvert^2$ | $i\frac{1}{v^2}(k_1 \cdot k_2)$ |

Table 1: Feynman Rules for the High Energy Lagrangian

| **Diagram** | **Lagrangian Term** | **Feynman Rule** |
|---|---|---|
| 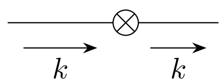  | $-(Z_\chi-1)\frac{1}{2}\lvert\partial\chi\rvert^2$ <br> $-(Z_\lambda Z_v^2 Z_\chi-1)\frac{\lambda v^2}{2}\chi^2$ | $i\left[(Z_\chi-1)k^2-(Z_\lambda Z_v^2 Z_\chi-1)\lambda v^2\right]$ |
| 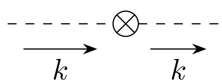  | $-(Z_\xi-1)\frac{1}{2}\lvert\partial\xi\rvert^2$ | $i(Z_\xi-1)k^2$ |
| 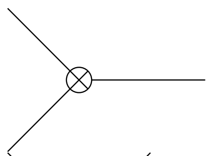 | $-(Z_\lambda Z_v Z_\chi^{3/2}-1)\frac{\lambda v}{2\sqrt{2}}\chi^3$ | $-i(Z_\lambda Z_v Z_\chi^{3/2}-1)\frac{3\lambda v}{\sqrt{2}}$ |
| 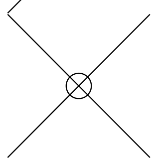 | $-(Z_\lambda Z_\chi^2-1)\frac{\lambda}{16}\chi^4$ | $-i(Z_\lambda Z_\chi^2-1)\frac{3\lambda}{2}$ |
| 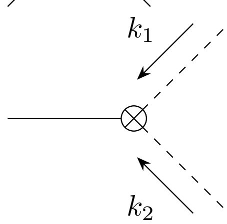  | $-(Z_v^{-1}Z_\chi^{1/2}Z_\xi-1)\frac{1}{\sqrt{2}v}\chi\lvert\partial\xi\rvert^2$ | $(Z_v^{-1}Z_\chi^{1/2}Z_\xi-1)i\frac{\sqrt{2}}{v}(k_1\cdot k_2)$ |
| 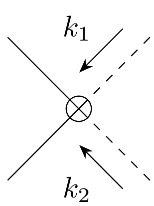  | $-(Z_v^{-2}Z_\chi Z_\xi-1)\frac{1}{4v^2}\chi^2\lvert\partial\xi\rvert^2$ | $(Z_v^{-2}Z_\chi Z_\xi-1)i\frac{1}{v^2}(k_1\cdot k_2)$ |

Table 2: Feynman Rules for Counterterms of the High Energy Lagrangian

Fortunately, it is unnecessary to derive all $Z$-factors from propagator and vertex corrections. All we need is the renormalized amplitude sufficient to determine the three independent Wilsonian coefficients $c_1, c_2, c_3$ from equation (36). Even though it is insufficient to determine $c_3$, we select the amplitude of $\xi\xi \to \xi\xi$ scattering for simplicity. A more complex six-point scattering amplitude, such as $\xi\xi\xi \to \xi\xi\xi$ or $\xi\xi \to \xi\xi\xi\xi$, is required for the identification of $c_3$.

Recall that our precision selection is order up to $\mathcal{O}(\lambda^2)$. Let us begin with the tree-level diagrams.

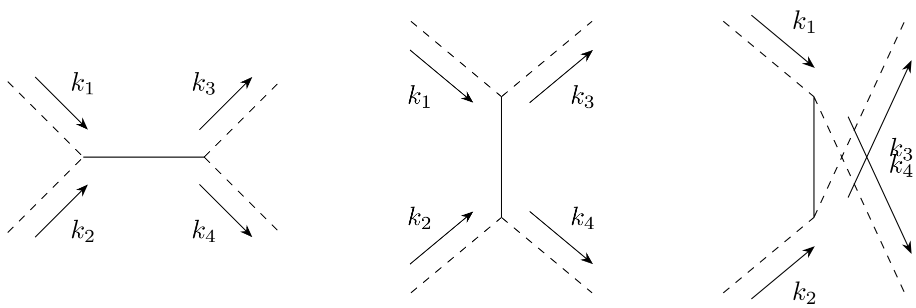


$$i\mathcal{M}_{11} = i \cdot [i\frac{\sqrt{2}}{v}(k_1 \cdot k_2)] \cdot [i\frac{\sqrt{2}}{v}(k_3 \cdot k_4)] \cdot [\frac{-i}{(k_1 + k_2)^2 + \lambda v^2 - i\epsilon}] \tag{41}$$

$$= -\lambda \frac{2(k_1 \cdot k_2)(k_3 \cdot k_4)}{M^4} \left\{ 1 - \frac{(k_1 + k_2)^2}{M^2} \right\} + \mathcal{O}((p_s/M)^8) \tag{42}$$

$$i\mathcal{M}_{12} = i \cdot [i\frac{\sqrt{2}}{v}(-k_1 \cdot k_3)] \cdot [i\frac{\sqrt{2}}{v}(-k_2 \cdot k_4)] \cdot [\frac{-i}{(k_1 - k_3)^2 + \lambda v^2 - i\epsilon}] \tag{43}$$

$$= -\lambda \frac{2(k_1 \cdot k_3)(k_2 \cdot k_4)}{M^4} \left\{ 1 - \frac{(k_1 - k_3)^2}{M^2} \right\} + \mathcal{O}((p_s/M)^8) \tag{44}$$

$$i\mathcal{M}_{13} = i \cdot [i\frac{\sqrt{2}}{v}(-k_1 \cdot k_4)] \cdot [i\frac{\sqrt{2}}{v}(-k_2 \cdot k_3)] \cdot [\frac{-i}{(k_1 - k_4)^2 + \lambda v^2 - i\epsilon}] \tag{45}$$

$$= -\lambda \frac{2(k_1 \cdot k_4)(k_2 \cdot k_3)}{M^4} \left\{ 1 - \frac{(k_1 - k_4)^2}{M^2} \right\} + \mathcal{O}((p_s/M)^8) \tag{46}$$

Mandelstam variables are a useful substitution for simplifying the amplitude.

$$s = (k_1 + k_2)^2 = 2k_1 \cdot k_2 = 2k_3 \cdot k_4, \tag{47}$$

$$t = (k_1 - k_3)^2 = -2k_1 \cdot k_3 = -2k_2 \cdot k_4, \tag{48}$$

$$u = (k_1 - k_4)^2 = -2k_1 \cdot k_4 = -2k_2 \cdot k_3. \tag{49}$$

The final tree-level amplitude is as follows:

$$i\mathcal{M}_1 = -\frac{\lambda}{2M^4}(s^2 + t^2 + u^2) + \frac{\lambda}{2M^6}(s^3 + t^3 + u^3) + \mathcal{O}((p_s/M)^8). \tag{50}$$

At order $\mathcal{O}(\lambda^2)$, 1-loop diagrams and counterterm diagrams are possible. There are a total of 42 possible 1-loop diagrams and 9 possible counterterm diagrams. However, only 13 diagrams are topologically independent, and each of them is duplicated by the $s$, $t$, and $u$ channels. Unless otherwise mentioned, one diagram has three accompanying channels. The notation $i\mathcal{M}^s$ represents the contribution calculated only with respect to the $s$-channel.

The first group consists of diagrams with $\xi$ loops.

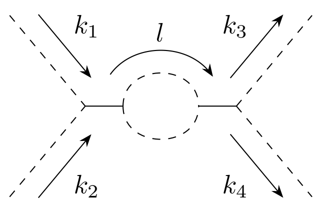


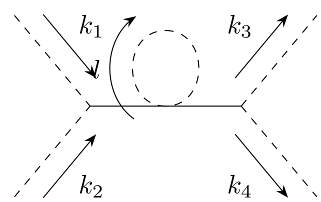


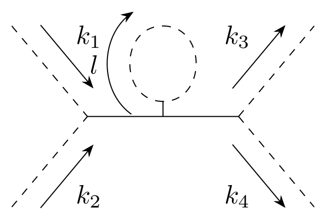


$$i\mathcal{M}_{21} \sim \frac{s^4}{M^8} \int \frac{d^d l}{(2\pi)^d} \frac{1}{(l^2 - i\epsilon)(\{l - (k_1 + k_2)\}^2 - i\epsilon)} = \mathcal{O}((p_s/M)^8) \tag{51}$$

$$i\mathcal{M}_{22} \sim \int \frac{d^d l}{(2\pi)^d} \frac{l^2}{l^2 - i\epsilon} = 0 \tag{52}$$

$$i\mathcal{M}_{23} \sim \int \frac{d^d l}{(2\pi)^d} \frac{l^2}{l^2 - i\epsilon} = 0 \tag{53}$$

The next group consists of the $\chi$-loop diagrams. Exceptionally, the second diagram has a total of six distinct contributions because it has no horizontal symmetry.

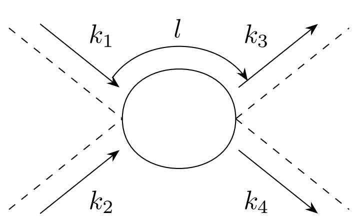


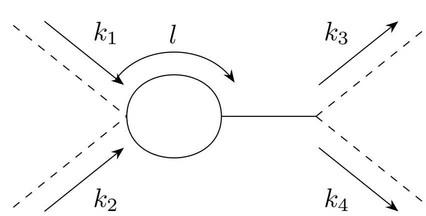

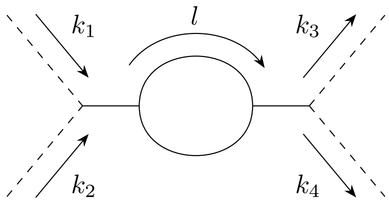


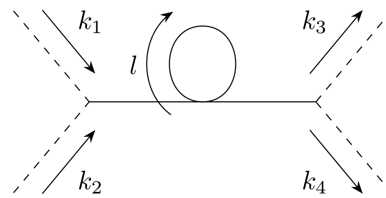


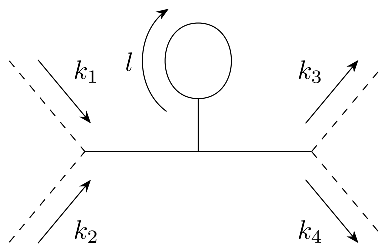


$$i\mathcal{M}_{24}^{s} = i \cdot \int \frac{d^d l}{(2\pi)^d} \cdot [i\frac{1}{v^2}(k_1 \cdot k_2)] \cdot [i\frac{1}{v^2}(k_3 \cdot k_4)] \cdot [\frac{-i}{l^2 + \lambda v^2 - i\epsilon}] \cdot [\frac{-i}{\{l-(k_1+k_2)\}^2 + \lambda v^2 - i\epsilon}] \tag{54}$$

$$= \frac{i\lambda^2 s^2}{M^4} \int \frac{d^d l}{(2\pi)^d} \frac{1}{(l^2 + M^2 - i\epsilon)(\{l-(k_1+k_2)\}^2 + M^2 - i\epsilon)} \tag{55}$$

$$= \frac{i\lambda^2 s^2}{M^4} \left[ \frac{i}{16\pi^2} \left( \frac{1}{\bar{\epsilon}} - \frac{s}{6M^2} - \log \frac{M^2}{\mu^2} \right) \right] + \mathcal{O}((p_s/M)^8) \tag{56}$$

$$i\mathcal{M}_{24} = \frac{\lambda^2}{16\pi^2 M^4} \left( -\frac{1}{\bar{\epsilon}} + \log \frac{M^2}{\mu^2} \right) (s^2 + t^2 + u^2) + \frac{\lambda^2}{96\pi^2 M^6}(s^3 + t^3 + u^3) + \mathcal{O}((p_s/M)^8) \tag{57}$$

$$i\mathcal{M}_{25}^{s} = i \cdot \int \frac{d^d l}{(2\pi)^d} [i\frac{1}{v^2}(k_1 \cdot k_2)] \cdot [-i\frac{3\lambda v}{\sqrt{2}}] \cdot [i\frac{\sqrt{2}}{v}(k_3 \cdot k_2)] \cdot [\frac{-i}{l^2 + \lambda v^2 - i\epsilon}] \cdot \tag{58}$$

$$[\frac{-i}{\{l-(k_1+k_2)\}^2 + \lambda v^2 - i\epsilon}] \cdot [\frac{-i}{(k_3+k_4)^2 + \lambda v^2 - i\epsilon}] \tag{59}$$

$$= -\frac{3i\lambda^2 s^2}{4M^2(s+M^2)} \int \frac{d^d l}{(2\pi)^d} \frac{1}{(l^2 + M^2 - i\epsilon)(\{l-(k_1+k_2)\}^2 + M^2 - i\epsilon)} \tag{60}$$

$$= \frac{3i\lambda^2 s^2}{4M^4} \left( 1 - \frac{s}{M^2} \right) \left[ \frac{i}{16\pi^2} \left( \frac{1}{\bar{\epsilon}} - \frac{s}{6M^2} - \log \frac{M^2}{\mu^2} \right) \right] + \mathcal{O}((p_s/M)^8) \tag{61}$$

$$i\mathcal{M}_{25} = \frac{3\lambda^2}{32\pi^2 M^4} \left( \frac{1}{\bar{\epsilon}} - \log \frac{M^2}{\mu^2} \right) (s^2 + t^2 + u^2) + \tag{62}$$

$$\frac{3\lambda^2}{32\pi^2 M^6}\left(-\frac{1}{\bar{\epsilon}}+\log\frac{M^2}{\mu^2}-\frac{1}{6}\right)(s^3+t^3+u^3)+\mathcal{O}((p_s/M)^8) \tag{63}$$

$$i\mathcal{M}^s_{26} = i\cdot\int\frac{d^dl}{(2\pi)^d}[i\frac{\sqrt{2}}{v}(k_1\cdot k_2)]\cdot[i\frac{\sqrt{2}}{v}(k_3\cdot k_4)]\cdot[-i\frac{3\lambda v}{\sqrt{2}}]^2\cdot \tag{64}$$

$$[\frac{-i}{(k_1+k_2)^2+\lambda v^2-i\epsilon}]^2\cdot[\frac{-i}{l^2+\lambda v^2-i\epsilon}]\cdot[\frac{-i}{\{l-(k_1+k_2)\}^2+\lambda v^2-i\epsilon}] \tag{65}$$

$$= \frac{9i\lambda^2 s^2}{4(s+M^2)^2}\int\frac{d^dl}{(2\pi)^d}\frac{1}{(l^2+M^2-i\epsilon)(\{l-(k_1+k_2)\}^2+M^2-i\epsilon)} \tag{66}$$

$$= \frac{9i\lambda^2 s^2}{4M^4}\left(1-2\frac{s}{M^2}\right)\left[\frac{i}{16\pi^2}\left(\frac{1}{\bar{\epsilon}}-\frac{s}{6M^2}-\log\frac{M^2}{\mu^2}\right)\right]+\mathcal{O}((p_s/M)^8) \tag{67}$$

$$i\mathcal{M}_{26} = -\frac{9\lambda^2}{64\pi^2 M^4}\left(\frac{1}{\bar{\epsilon}}-\log\frac{M^2}{\mu^2}\right)(s^2+t^2+u^2)- \tag{68}$$

$$\frac{9\lambda^2}{64\pi^2 M^6}\left(-\frac{2}{\bar{\epsilon}}+2\log\frac{M^2}{\mu^2}-\frac{1}{6}\right)(s^3+t^3+u^3)+\mathcal{O}((p_s/M)^8) \tag{69}$$

$$i\mathcal{M}^s_{27} = i\cdot\int\frac{d^dl}{(2\pi)^d}[i\frac{\sqrt{2}}{v}(k_1\cdot k_2)]\cdot[i\frac{\sqrt{2}}{v}(k_3\cdot k_4)]\cdot[-i\frac{3\lambda}{2}]\cdot[\frac{-i}{(k_1+k_2)^2+\lambda v^2-i\epsilon}]^2\cdot[\frac{-i}{l^2+\lambda v^2-i\epsilon}] \tag{70}$$

$$= -\frac{3i\lambda^2 s^2}{4M^2(s+M^2)^2}\int\frac{d^dl}{(2\pi)^d}\frac{1}{l^2+M^2-i\epsilon} \tag{71}$$

$$= -\frac{3i\lambda^2 s^2}{4M^6}\left(1-\frac{2s}{M^2}\right)\left[-\frac{iM^2}{16\pi^2}\left(\frac{1}{\bar{\epsilon}}+1-\log\frac{M^2}{\mu^2}\right)\right]+\mathcal{O}((p_s/M)^8) \tag{72}$$

$$i\mathcal{M}_{27} = -\frac{3\lambda^2}{64\pi^2 M^4}\left(\frac{1}{\bar{\epsilon}}+1-\log\frac{M^2}{\mu^2}\right)(s^2+t^2+u^2)- \tag{73}$$

$$\frac{3\lambda^2}{64\pi^2 M^6}\left(\frac{1}{\bar{\epsilon}}+1-\log\frac{M^2}{\mu^2}\right)(s^3+t^3+u^3)+\mathcal{O}((p_s/M)^8) \tag{74}$$

$$i\mathcal{M}^s_{28} = i\cdot\int\frac{d^dl}{(2\pi)^d}[i\frac{\sqrt{2}}{v}(k_1\cdot k_2)]\cdot[i\frac{\sqrt{2}}{v}(k_3\cdot k_4)]\cdot[-i\frac{3\lambda v}{\sqrt{2}}]^2\cdot \tag{75}$$

$$[\frac{-i}{(k_1+k_2)^2+\lambda v^2-i\epsilon}]^2\cdot[\frac{-i}{\lambda v^2-i\epsilon}]\cdot[\frac{-i}{l^2+\lambda v^2-i\epsilon}] \tag{76}$$

$$= \frac{9i\lambda^2 s^2}{4M^2(s+M^2)^2}\int\frac{d^dl}{(2\pi)^d}\frac{1}{l^2+M^2-i\epsilon} \tag{77}$$

$$= \frac{9i\lambda^2 s^2}{4M^6}\left(1-\frac{2s}{M^2}\right)\left[-\frac{iM^2}{16\pi^2}\left(\frac{1}{\bar{\epsilon}}+1-\log\frac{M^2}{\mu^2}\right)\right]+\mathcal{O}((p_s/M)^8) \tag{78}$$

$$i\mathcal{M}_{28} = \frac{9\lambda^2}{64\pi^2 M^4}\left(\frac{1}{\bar{\epsilon}}+1-\log\frac{M^2}{\mu^2}\right)(s^2+t^2+u^2)+ \tag{79}$$

$$\frac{9\lambda^2}{64\pi^2 M^6}\left(\frac{1}{\bar{\epsilon}}+1-\log\frac{M^2}{\mu^2}\right)(s^3+t^3+u^3)+\mathcal{O}((p_s/M)^8) \tag{80}$$

There are three topologically independent diagrams with mixed loops. The second and third diagrams exceptionally have six distinct contributions each, because they have no horizontal symmetry.

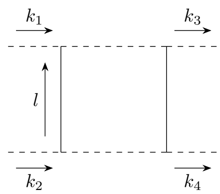


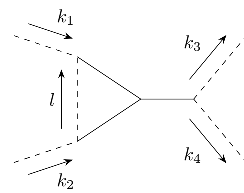


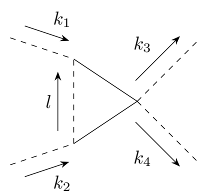


$$i\mathcal{M}^s_{29} = i\cdot\int\frac{d^dl}{(2\pi)^d}[-i\frac{\sqrt{2}}{v}\{k_1\cdot(k_1+l)\}]\cdot[-i\frac{\sqrt{2}}{v}\{(k_1+l)\cdot k_3\}]\cdot \tag{81}$$

$$[-i\frac{\sqrt{2}}{v}\{k_2\cdot(k_2-l)\}]\cdot[-i\frac{\sqrt{2}}{v}\{(k_2-l)\cdot k_4\}]\cdot[\frac{-i}{l^2+\lambda v^2-i\epsilon}]\cdot \tag{82}$$

$$[\frac{-i}{(k_1-k_3+l)^2+\lambda v^2-i\epsilon}]\cdot[\frac{-i}{(k_1+l)^2-i\epsilon}]\cdot[\frac{-i}{(k_2-l)^2-i\epsilon}] \tag{83}$$

$$=\frac{4i\lambda^2}{M^4}\int\frac{d^dl}{(2\pi)^d}\frac{\{k_1\cdot(k_1+l)\}\{(k_1+l)\cdot k_3\}\{k_2\cdot(k_2-l)\}\{(k_2-l)\cdot k_4\}}{(l^2+M^2-i\epsilon)\{(l+k_1-k_3)^2+M^2-i\epsilon\}\{(l+k_1)^2-i\epsilon\}\{(l-k_2)^2-i\epsilon\}} \tag{84}$$

$$=\frac{\lambda^2}{192\pi^2M^4}\left(\frac{1}{\bar{\epsilon}}-\log\frac{M^2}{\mu^2}+\frac{5}{6}\right)(st+su+tu)+ \tag{85}$$

$$\frac{\lambda^2}{\pi^2M^6}\left[-\frac{s^2t}{768}-\frac{s^2u}{512}-\frac{st^2}{768}+\frac{su^2}{512}+\frac{stu}{1152}-\frac{t^2u}{512}-\frac{tu^2}{1536}\right]+\mathcal{O}((p_s/M)^8) \tag{86}$$

$$i\mathcal{M}_{29} = -\frac{\lambda^2}{64\pi^2M^4}\left(\frac{1}{\bar{\epsilon}}-\log\frac{M^2}{\mu^2}+\frac{5}{6}\right)(s^2+t^2+u^2) \tag{87}$$

$$+\frac{\lambda^2}{144\pi^2M^6}(s^3+t^3+u^3)+\mathcal{O}\big((p_s/M)^8\big) \tag{88}$$

$$i\mathcal{M}^s_{2,10} = i\cdot\int\frac{d^dl}{(2\pi)^d}[i\frac{\sqrt{2}}{v}(l\cdot k_1)]\cdot[-i\frac{\sqrt{2}}{v}(l\cdot k_2)]\cdot[i\frac{\sqrt{2}}{v}(k_3\cdot k_4)]\cdot[-i\frac{3\lambda v}{\sqrt{2}}]\cdot[\frac{-i}{l^2-i\epsilon}]\cdot \tag{89}$$

$$[\frac{-i}{(l+k_1)^2+\lambda v^2-i\epsilon}]\cdot[\frac{-i}{(l-k_2)^2+\lambda v^2-i\epsilon}]\cdot[\frac{-i}{(k_3+k_4)^2+\lambda v^2-i\epsilon}] \tag{90}$$

$$= \frac{3i\lambda^2 s}{M^2(s+M^2)}\int\frac{d^dl}{(2\pi)^d}\frac{(l\cdot k_1)(l\cdot k_2)}{(l^2-i\epsilon)\{(l+k_1)^2+M^2-i\epsilon\}\{(l-k_2)^2+M^2-i\epsilon\}\}} \tag{91}$$

$$= \frac{3i\lambda^2 s}{M^4}\left(1-\frac{s}{M^2}\right)\left[\frac{is}{128\pi^2}\left(\frac{1}{\epsilon}+\frac{1}{2}-\log\frac{M^2}{\mu^2}\right)-\frac{is^2}{576\pi^2M^2}\right]\mathcal{O}((p_s/M)^8) \tag{92}$$

$$i\mathcal{M}_{2,10} = -\frac{3\lambda^2}{64\pi^2M^4}\left(\frac{1}{\epsilon}+\frac{1}{2}-\log\frac{M^2}{\mu^2}\right)(s^2+t^2+u^2)+ \tag{93}$$

$$\frac{3\lambda^2}{64\pi^2M^6}\left(\frac{1}{\epsilon}+\frac{13}{18}-\log\frac{M^2}{\mu^2}\right)(s^3+t^3+u^3)+\mathcal{O}((p_s/M)^8) \tag{94}$$

$$i\mathcal{M}^s_{2,11} = i\cdot\int\frac{d^dl}{(2\pi)^d}[i\frac{\sqrt{2}}{v}(l\cdot k_1)]\cdot[-i\frac{\sqrt{2}}{v}(l\cdot k_2)]\cdot[i\frac{1}{v^2}(k_3\cdot k_4)]\cdot \tag{95}$$

$$[\frac{-i}{l^2-i\epsilon}]\cdot[\frac{-i}{(l+k_1)^2+\lambda v^2-i\epsilon}]\cdot[\frac{-i}{(l-k_2)^2+\lambda v^2-i\epsilon}] \tag{96}$$

$$= -\frac{i\lambda^2 s}{M^4}\int\frac{d^dl}{(2\pi)^d}\frac{(l\cdot k_1)(l\cdot k_2)}{(l^2-i\epsilon)\{(l+k_1)^2+M^2-i\epsilon\}\{(l-k_2)^2+M^2-i\epsilon\}\}} \tag{97}$$

$$= -\frac{i\lambda^2 s}{M^4}\left[\frac{is}{128\pi^2}\left(\frac{1}{\epsilon}+\frac{1}{2}-\log\frac{M^2}{\mu^2}\right)-\frac{is^2}{576\pi^2M^2}\right]\mathcal{O}((p_s/M)^8) \tag{98}$$

$$i\mathcal{M}_{2,11} = \frac{\lambda^2}{64\pi^2M^4}\left(\frac{1}{\epsilon}+\frac{1}{2}-\log\frac{M^2}{\mu^2}\right)(s^2+t^2+u^2)- \tag{99}$$

$$\frac{\lambda^2}{576\pi^2M^6}(s^3+t^3+u^3)+\mathcal{O}((p_s/M)^8) \tag{100}$$

The final counterterms are simply the ones modified from the tree-level diagram. However, the first diagram has six distinct contributions due to the asymmetry.

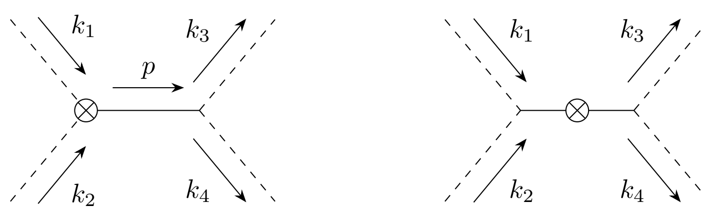


$$i\mathcal{M}^s_{2,12} = -(Z_v^{-1}Z_\chi^{1/2}Z_\xi-1)\frac{\lambda s^2}{2M^4}\left\{1-\frac{s}{M^2}\right\}+\mathcal{O}((p_s/M)^8) \tag{101}$$

$$i\mathcal{M}_{2,12} = -(Z_v^{-1}Z_\chi^{1/2}Z_\xi-1)\frac{\lambda}{M^4}(s^2+t^2+u^2)+(Z_v^{-1}Z_\chi^{1/2}Z_\xi-1)\frac{\lambda}{M^6}(s^3+t^3+u^3)+\mathcal{O}((p_s/M)^8) \tag{102}$$

$$i\mathcal{M}^s_{2,13} = i \cdot [i\frac{\sqrt{2}}{v}(k_1 \cdot k_2)] \cdot [i\frac{\sqrt{2}}{v}(k_3 \cdot k_4)] \cdot [i(Z_\chi - 1)(k_1 + k_2)^2 - i(Z_\lambda Z_v^2 Z_\chi - 1)M^2] \tag{103}$$

$$= \frac{\lambda s^2}{2M^2}\left\{\frac{Z_\chi - 1}{2}s - (Z_\lambda Z_v^2 Z_\chi - 1)M^2\right\} \tag{104}$$

$$i\mathcal{M}_{2,13} = \frac{(Z_\chi - 1)\lambda}{4M^2}(s^3 + t^3 + u^3) - \frac{(Z_\lambda Z_v^2 Z_\chi - 1)\lambda}{2}(s^2 + t^2 + u^2) \tag{105}$$

The role of the $Z$-factors is clear. They only absorb all $1/\bar{\epsilon} = 1/\epsilon - \gamma + \log 4\pi$ divergences in the coefficients of $(s^2+t^2+u^2)$ and $(s^3+t^3+u^3)$ for $i\sum_{n=1}^{11}\mathcal{M}_{2,n}$, provided the selection of minimal subtraction scheme ($\overline{\text{MS}}$). Therefore, the following is the total 1-loop $\xi\xi \to \xi\xi$ scattering amplitude in the high-energy theory.

$$i\mathcal{M}_2 = \frac{\lambda^2}{16\pi^2 M^4}\left(\frac{25}{24} + \log\frac{M^2}{\mu^2}\right)(s^2 + t^2 + u^2) + \tag{106}$$

$$\frac{\lambda^2}{\pi^2 M^6}\left(\frac{29}{192} - \frac{21}{64}\log\frac{M^2}{\mu^2}\right)(s^3 + t^3 + u^3) + \mathcal{O}((p_s/M)^8) \tag{107}$$

## 4.3 EFT Amplitude Calculation

The effective Lagrangian up to order $\mathcal{O}((p_s/M)^6)$ can be similarly expanded with appropriate $Z$-factors to renormalize the bare quantities: $\xi_0 = \sqrt{Z_\xi}\xi$, $c_{10} = Z_1 c_1$, $c_{20} = Z_2 c_2$, and $c_{30} = Z_3 c_3$. Then, the expansion becomes as follows.

$$\mathcal{L}_{\text{eff}}(\xi) = -\frac{1}{2}\partial^\mu\xi\partial_\mu\xi + \frac{1}{8}c_1(\partial^\mu\xi\partial_\mu\xi)^2 + \frac{1}{4}c_2(\partial^\mu\xi\partial_\mu\xi)\Box(\partial^\nu\xi\partial_\nu\xi) + \frac{1}{48}c_3(\partial^\mu\xi\partial_\mu\xi)^3 \tag{108}$$

$$\mathcal{L}_{\text{eff},ct}(\xi) = -(Z_\xi - 1)\frac{1}{2}\partial^\mu\xi\partial_\mu\xi + (Z_\xi^2 Z_1 - 1)\frac{1}{8}c_1(\partial^\mu\xi\partial_\mu\xi)^2 \tag{109}$$

$$+ (Z_\xi^2 Z_2 - 1)\frac{1}{4}c_2(\partial^\mu\xi\partial_\mu\xi)\Box(\partial^\nu\xi\partial_\nu\xi) + (Z_\xi^3 Z_3 - 1)\frac{1}{48}c_3(\partial^\mu\xi\partial_\mu\xi)^3 \tag{110}$$

The following are its Feynman rules.

| **Diagram** | **Lagrangian Term** | **Feynman Rule** |
|---|---|---|
| 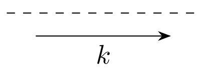 | $-\frac{1}{2}\partial^\mu\xi\partial_\mu\xi$ | $\frac{-i}{k^2-i\epsilon}$ |
| 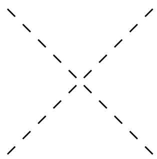 | $\frac{1}{8}c_1(\partial^\mu\xi\partial_\mu\xi)^2$ $+\frac{1}{4}c_2(\partial^\mu\xi\partial_\mu\xi)\Box(\partial^\nu\xi\partial_\nu\xi)$ | $ic_1\sum_{\text{3 perms}}(k_i\cdot k_j)(k_k\cdot k_l)$ $-ic_2\sum_{\text{6 perms}}(k_i\cdot k_j)(k_k\cdot k_l)(k_k+k_l)^2$ |
| 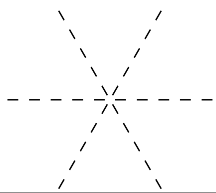 | $\frac{1}{48}c_3(\partial^\mu\xi\partial_\mu\xi)^3$ | $-\,ic_3\sum_{\text{15 perms}}(k_i\cdot k_j)(k_k\cdot k_l)(k_m\cdot k_n)$ |

Table 3: Feynman Rules for the Effective Lagrangian

| **Diagram** | **Lagrangian Term** | **Feynman Rule** |
|---|---|---|
| 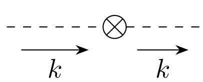 | $-(Z_\xi-1)\frac{1}{2}\partial^\mu\xi\partial_\mu\xi$ | $i(Z_\xi-1)k^2$ |
| 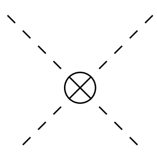 | $(Z_\xi^2Z_1-1)\frac{1}{8}c_1(\partial^\mu\xi\partial_\mu\xi)^2$ $+(Z_\xi^2Z_2-1)\frac{1}{4}c_2(\partial^\mu\xi\partial_\mu\xi)\Box(\partial^\nu\xi\partial_\nu\xi)$ | $(Z_\xi^2Z_1-1)\times(\text{Bare } c_1 \text{ Rule})$ $+(Z_\xi^2Z_2-1)\times(\text{Bare } c_2 \text{ Rule})$ |
| 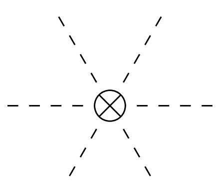 | $(Z_\xi^3Z_3-1)\frac{1}{48}c_3(\partial^\mu\xi\partial_\mu\xi)^3$ | $(Z_\xi^3Z_3-1)\times(\text{Bare } c_3 \text{ Rule})$ |

Table 4: Feynman Rules for the Counterterm of Effective Lagrangian

Again, since our chosen precision goal includes one-loop corrections, let us begin with the tree-level diagram. There is only one tree-level diagram for $\xi\xi \to \xi\xi$ scattering.

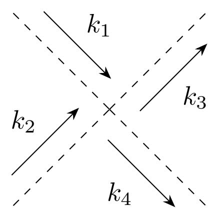


This single diagram gives the amplitude below.

$$i\mathcal{M}_{\mathrm{eff},1} = i \cdot [ic_1 \sum_{3\text{ perms}} (k_i \cdot k_j)(k_k \cdot k_l) - ic_2 \sum_{6\text{ perms}} (k_i \cdot k_j)(k_k \cdot k_l)(k_k + k_l)^2] \tag{111}$$

$$= -\frac{c_1}{4}(s^2 + t^2 + u^2) + \frac{c_2}{2}(s^3 + t^3 + u^3) \tag{112}$$

At order $\mathcal{O}(\lambda^2)$, there are two topologically independent one-loop diagrams and one counterterm diagram. The loop diagrams have three degeneracies, corresponding to the $s$, $t$, and $u$ channels.

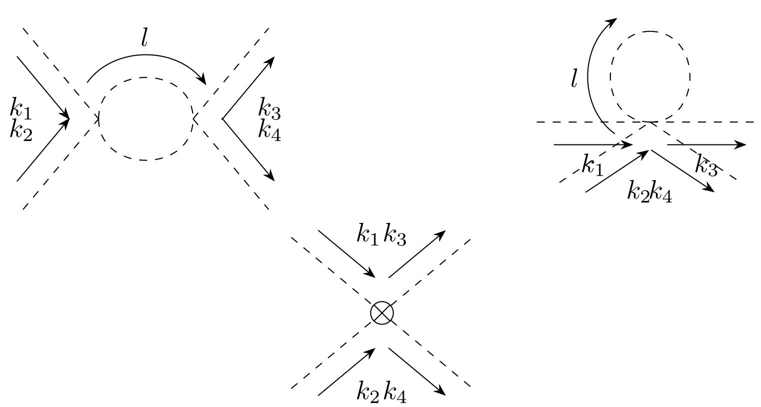


$$i\mathcal{M}_{\mathrm{eff},21} \sim \frac{s^4}{M^8} \int \frac{d^d l}{(2\pi)^d} \frac{1}{(l^2 - i\epsilon)(\{l - (k_1 + k_2)\}^2 - i\epsilon)} = \mathcal{O}((p_s/M)^8) \tag{113}$$

$$i\mathcal{M}_{\mathrm{eff},22} \sim \int \frac{d^d l}{(2\pi)^d} \frac{l^2}{(l^2 - i\epsilon)} = 0 \tag{114}$$

$$i\mathcal{M}_{\mathrm{eff},23} = i \cdot [i(Z_\xi^2 Z_1 - 1)c_1 \sum_{3\text{ perms}} (k_i \cdot k_j)(k_k \cdot k_l) - i(Z_\xi^2 Z_2 - 1)c_2 \sum_{6\text{ perms}} (k_i \cdot k_j)(k_k \cdot k_l)(k_k + k_l)^2] \tag{115}$$

Since there is no divergence to deal with, the total amplitude at order $\mathcal{O}(\lambda^2)$ is simply of order $\mathcal{O}((p_s/M)^8)$.

$$i\mathcal{M}_{\text{eff},2} = \mathcal{O}((p_s/M)^8). \tag{116}$$

## 4.4 Matching

Now, the final procedure is straightforward. We match the $\xi\xi \to \xi\xi$ scattering amplitudes in the high-energy theory and in the EFT to obtain the Wilson coefficients up to order $\mathcal{O}((p_s/M)^6)$ and $\mathcal{O}(\lambda^2)$.

Starting with the tree-level amplitudes at order $\mathcal{O}(\lambda)$, the results calculated in the previous sections are the following, where $c_1^{(0)}, c_2^{(0)}$ are the first orders of Wilson coefficients.

$$i\mathcal{M}_1 = -\frac{\lambda}{2M^4}(s^2+t^2+u^2) + \frac{\lambda}{2M^6}(s^3+t^3+u^3), \tag{117}$$

$$i\mathcal{M}_{\text{eff},1}^{(0)} = -\frac{c_1^{(0)}}{4}(s^2+t^2+u^2) + \frac{c_2^{(0)}}{2}(s^3+t^3+u^3). \tag{118}$$

Both results must be identical as functions of the kinematic variables $s, t, u$. The only possible values for the first order Wilsonian coefficients $c_1^{(0)}$ and $c_2^{(0)}$ are therefore as follows. As mentioned before, $c_3$ cannot be determined from the four-point amplitude.

$$c_1^{(0)} = \frac{2\lambda}{M^4} \tag{119}$$

$$c_2^{(0)} = \frac{\lambda}{M^6} \tag{120}$$

After matching the amplitude at order $\mathcal{O}(\lambda^2)$, the next-order Wilsonian coefficients $c_1^{(1)}$ and $c_2^{(1)}$ must compensate for the one-loop diagrams in the high-energy theory.

$$\begin{aligned} i\mathcal{M}_2 = {} & \frac{\lambda^2}{16\pi^2 M^4}\left(\frac{25}{24} + \log\frac{M^2}{\mu^2}\right)(s^2+t^2+u^2) \\ & + \frac{\lambda^2}{\pi^2 M^6}\left(\frac{29}{192} - \frac{21}{64}\log\frac{M^2}{\mu^2}\right)(s^3+t^3+u^3), \end{aligned} \tag{121}$$

$$i\mathcal{M}_{\text{eff},1}^{(1)} = -\frac{c_1^{(1)}}{4}(s^2+t^2+u^2) + \frac{c_2^{(1)}}{2}(s^3+t^3+u^3). \tag{122}$$

By this final matching, we can identify $c_1^{(1)}$ and $c_2^{(1)}$, which depend on $\mu$. In a complete EFT calculation, it is compensated by the EFT running and loop contributions, so that physical amplitudes are independent of $\mu$.

$$c_1^{(1)} = -\frac{\lambda^2}{4\pi^2 M^4}\left(\frac{25}{24} + \log\frac{M^2}{\mu^2}\right) \tag{123}$$

$$c_2^{(1)} = \frac{\lambda^2}{\pi^2 M^6}\left(\frac{29}{96} - \frac{21}{32}\log\frac{M^2}{\mu^2}\right) \tag{124}$$

Finally, it is possible to determine the Wilsonian coefficients $c_1$ and $c_2$ up to order $\mathcal{O}(\lambda^2)$:

$$c_1 = \frac{2\lambda}{M^4} - \frac{\lambda^2}{4\pi^2 M^4}\left(\frac{25}{24} + \log\frac{M^2}{\mu^2}\right) + \mathcal{O}(\lambda^3), \tag{125}$$

$$c_2 = \frac{\lambda}{M^6} + \frac{\lambda^2}{\pi^2 M^6}\left(\frac{29}{96} - \frac{21}{32}\log\frac{M^2}{\mu^2}\right) + \mathcal{O}(\lambda^3). \tag{126}$$

In order for the Wilsonian action to remain valid as a perturbative theory, we choose the arbitrary parameter $\mu$ to be of the scale $M$.

These coefficients are sufficient to identify the amplitude up to the precision limits $\mathcal{O}((p_s/M)^6)$ and $\mathcal{O}(\lambda^2)$, accompanied by $c_3$, which is obtained from six-point amplitude matching.

# 5 General Philosophy

The main point of this chapter is that it is not merely a fitting theory. There are some key philosophical aspects to the value of EFT.

First, the most straightforward and practical aspect is that it optimizes the number of calculations. Given a precision limit, we can deduce a theory that is just sufficient for every amplitude and physical quantity to match within that limit.

Second, the mechanism of EFT governs the number of independent parameters required to construct the desired theory. If we know the structure of the high-energy theory, as in the toy model example in Chapter 4, the number of parameters is far fewer than the number of Wilsonian coefficients. For example, in the toy model, there might be arbitrarily many finite Wilsonian coefficients if we enhance the precision goal. However, they are all formed from only two crucial quantities, $M$ and $\lambda$. Even though if we have no clue about the high-energy theory, it is possible to find the minimum number of parameters, which is each Wilsonian coefficient treated independently, needed for a fixed precision goal by power counting.

Third, it gives us a hint about the structure of the higher-energy theory. The dependence or ratio between the Wilsonian coefficients gives us strong constraints on how the high-energy theory must be shaped in order for the EFT to match it.

Lastly, this is the most intangible but important viewpoint. EFT changed the paradigm of how the subject of science must evolve. Before then, the aim of science was to build an absolute theory to explain all phenomena. If a counterexample appeared, we would fix the theory again and again to get closer to that goal. However, from the viewpoint of EFT, there is no such absolute theory. Every theory is merely an effective theory of some higher-hierarchy theory. We can expand our theory accompanied by higher precision and a wider range of experimental data.

# 6 Further Study Goals

The first further objective is to study how symmetries are inherited in EFT. In particular, anomaly matching would provide a useful criterion for checking whether the low-energy effective theory preserves the structure of the high-energy theory.

The second objective is to analyze weak interactions using EFT when the underlying high-energy theory is the Standard Model. This would clarify how heavy particles are integrated out and how their effects remain as local terms at low energy.

The third objective is to study the role of gravitons in EFT. Since gravity is non-renormalizable in the usual perturbative sense, EFT provides a systematic framework for treating quantum gravitational effects at low energies.

Finally, it would be useful to understand the Standard Model itself as an effective theory. This viewpoint allows possible higher-energy physics beyond the Standard Model to be encoded in higher-dimensional terms.